VII International Conference on Computational Methods for Coupled Problems in Science and Engineering
COUPLED PROBLEMS 2017
M. Papadrakakis, E. Oñate and B. Schrefler (Eds)

HIGH FIDELITY AERO-STRUCTURAL OPTIMIZATION OF A WING USING A STEP-RANGE APPROACH

PAOLO F. SCARAMUZZINO†, ANDREA SICILIANI† AND GIUSEPPE QUARANTA†

†Dipartimento di Scienze e Tecnologie Aerospaziali, Politecnico di Milano
Edifici B12, Campus Bovisa
via La Masa, 34 Milano 20156 Italy
email: giuseppe.quaranta@polimi.it

Key words: Multidisiciplinary Optimization, Wing Design, CFD, FEM, Brequet Range Formula

Abstract. This paper present the effect of using a more detailed model for the computation of the range, when it is used as objective for the multidiciplinary optimization of a transonic wing of a business jet. The new formulation considers the change of angle of attack that the aircraft must follow during cruise.

1 INTRODUCTION

The ever-growing realm of applications and the explosion in computing power is driving optimization research toward new and exciting directions. A considerable amount of research has been conducted on multidisciplinary design optimization (MDO) and its application to aircraft design [1, 2]. In most cases sound coupling and optimization methods were shown to be extremely important because some techniques, such as sequential discipline optimization, were unable to converge to the true optimum of a coupled system. Aerostructural analysis has traditionally been carried out in a cut-and-try basis. Aircraft designers have a preconceived idea of the shape of an optimal load distribution and then tailor the jig shape of the structure so that the deflected wing shape under a 1-g load gives the desired load distribution. Although this approach might suffice for conventional transport aircraft, for which there is considerable accumulated experience, in the case of either new planform concepts or new flight regimes the lack of experience combined with the complexities of aero-structural interactions can lead to designs that are far from optimal. The objective of this work is to develop an MDO framework for high fidelity analysis and optimization of aircraft configurations. The paper presents the current capability of this framework through the aerostructural design of a transonic business-jet wing. This paper focuses on the demonstration of an integrated aero-structural method

for the design of aerospace vehicles. Both aerodynamics and structures are represented using high-fidelity models. The aerodynamic outer-mold line and the structure, with a fixed topology, are parameterized using a large number of design variables. The aerodynamic sensitivities with respect to outer-mold line shape variables are computed using an accurate and efficient adjoint procedure. The structural sensitivities with respect to structural design variables are computed using finite differences. The cross-gradients are evaluated analytically. Kreisselmeier Steinhauser [3] functions are used to reduce the number of structural constraints in the problem. Results of the aerodynamic shape and structural optimization for natural laminar-flow transonic business jet are presented.

The current approach to MDO applied to aircraft design uses the Breguet range equation as objective function [4]. This means that the variation of attitude during cruise, which is related to the loss of weight caused by fuel consumption, is not taken into account. The innovative approach presented in this work is to divide the cruise into several steps; over each step the attitude is considered to be constant, so that the Breguet range formula can be applied. The total range is then evaluated as the sum of the ranges of each step, leading to a sort of multi-objective optimization. The bigger is the number of step considered, the more accurate is the solution obtained. This new approach is called step-range and its results are compared with those obtained through sequential discipline optimization and single objective optimization.

2 NUMERICAL MODELS

In this section the numerical model employed to perform the optimization are presented.

2.1 Aerodynamic model

To investigate the effect of the application of the step-range approach, it has been decided to solve the optimization problem using for aerodynamic forces the inviscid Euler set of equation. This will limit the computational cost with respect to the viscous Navier-Stokes equations. Euler equations neglect fluid viscosity; this simplification fits well for very high Reynolds numbers. So, it could be considered an approximate yet sufficiently accurate model for an initial design through optimization.

The Euler equations are a set of three equations: two scalar and one vectorial:

$$\begin{cases} \frac{\partial \rho}{\partial t} + \boldsymbol{\nabla} \cdot (\rho \mathbf{u}) = 0 \\ \frac{\partial \rho \mathbf{u}}{\partial t} + \boldsymbol{\nabla} \cdot (\rho \mathbf{u} \otimes \mathbf{u} + P\mathbf{I}) = \mathbf{0} \\ \frac{\partial \rho E^t}{\partial t} + \boldsymbol{\nabla} \cdot [\mathbf{u}\,(E^t + P)] = 0 \end{cases} \tag{1}$$

where ρ is the density of the fluid, $\mathbf{u}$ is the velocity vector, P is the pressure, E^t is the total energy ($E^t = \rho e + \frac{1}{2}\rho \mathbf{u}^2$), where e is the specific internal energy) and $\mathbf{I}$ is the identity matrix.

This set of equations must be complemented with two equations of state, e.g.

$$P = P(e, \rho); \quad T = T(e, \rho) \tag{2}$$

As it will be discussed later, the optimization process is gradient based. This means that the gradient of the aerodynamics variables has to be calculated with respect to the design variables. Since the calculation of the gradients at each iteration would take a huge amount of computational time, the Euler equations are solved exploiting an adjoint formulation [5, 6] This leads to a significant reduction of the computational time.

2.1.1 Free Form Deformation

One of the most important points in the definition of a shape parametrization problem is the choice of the parametrization technique. A possible choice is the Free-Form Deformation (FFD) [7, 8]. The basic FFD concept is the deformation of a pre-existing object. This technique deforms a lattice that is built around the object and manipulates the whole space in which the object is embedded. The strong point of the method is that, by deforming the whole volume around the object, the computational grid is also being automatically deformed with the object itself. This feature makes the FFD technique preferable than others which only deform the object. In fact, in this case, the creation of a new computational grid has to be performed. This would lead to the growing of the computational cost. The lattice consists of an ordered mesh of control points and is placed in a way to wrap the object to be deformed. It defines a parametric coordinate system. The control points are used to approximate the curves that describe the object within the box. In particular, it is possible to define three different polynomials for each direction. Bézier curve have been chosen for the parametrization. These curves can be seen as a linear combination of Bernstein basis polynomials [9]. The CFD solver tool for grid deformation through Free-Form Deformation uses the Bzier method to approximate curves. It is possible to extend the Bézier curve into a Bézier box in the three dimension space using a trivariate Bernstein polynomial.

The wing, object of the optimization, has been embedded within a Free-Form Deformation box, as shown in Figure 1. The number of aerodynamic design variables depends on the approximating degree of the Bernstein polynomials. In table 1, the degrees of polynomials chosen in each direction are listed.

Cartesian Direction	**Polynomial Degree**	**No. of Control Points**
i	l = 10	11
j	m = 8	9
k	n = 1	2

Table 1: Description of aerodynamic design variables.

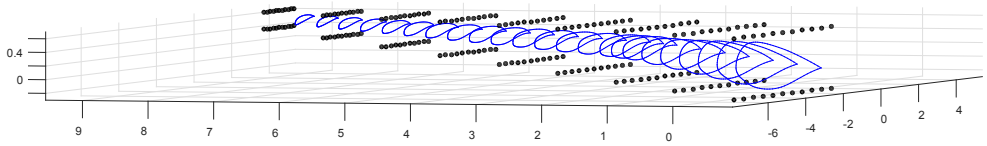

Figure 1: Free-Form Deformation box around the wing.

Hence, the total number of design variables is: $11 \times 9 \times 2 = 198$.

2.2 Structural model

There are several models available to describe the different behavior of a structural element. The choice of one of them depends on the level of accuracy required and on the fulfillment of the hypothesis at the basis of each model. In the preliminary design phase, the wing can be modeled as a beam since it usually has a large aspect ratio.

Knowing the wing layout in terms of number and type of stringers and of panels thickness, its bending and torsional stiffness can be evaluated through a semi-monocoque approach. In order to better reproduce wing torsional stiffness, some structural nodes are allocated spanwise in correspondence of leading and trailing edges and they are rigidly linked to beam axis nodes. In this way, it is possible to keep in consideration the contribute of the ribs.

The typical wing of business jet presents two changes in the sweep angle at trailing edge and so three different parts can be considered: root, center and tip. Each part has been discretized in a certain number of equally-spaced beam elements. Beam elements in CSM solver can be defined as tapered. This implies that the beam properties change along its axis and it can be done by defining different sections at the beginning and at the end of the element.

The beam properties are evaluated through the semi-monocoque approach, so they depend on the number and type of stringers and on panels thickness. If it is supposed that the resulting wing box is symmetric, it is necessary to define three design variables

for each beam section[1]: stringers area, spar webs thickness and skin panels thickness.

It is necessary to impose the continuity of the design variables between two consecutive beam elements, except for those across the sweep angle changes. Tab. 2 lists the number of design variables for each wing block.

Wing Block	**No. Elements**	**No. Design Variables**		
		Stringers Area	**Webs Thickness**	**Panels Thickness**
Root	6	7	7	7
Center	2	3	3	3
Tip	14	15	15	15
Total	22	25	25	25

Table 2: Description of structural design variables

3 WING AERO-STRUCTURAL DESIGN OPTIMIZATION

3.1 Step-range Breguet formulation

The typical multidisciplinary function that takes into account both aerodynamic and structural design aspects is represented by the *range formula*, first derived by Louis Charles Breguet [10].

$$\mathrm{d}R = \frac{V}{c_T}\frac{C_L}{C_D}\frac{1}{W}\,\mathrm{d}W \quad \Rightarrow \quad R = \frac{V}{c_T}\frac{C_L}{C_D}\ln\left(\frac{W_{in}}{W_{fin}}\right) \tag{3}$$

where R is the range, c_T is the specific fuel consumption, C_L is the lift coefficient, C_D is the drag coefficient, W_{in} is the initial weight and W_{fin} is the final weight.

In Eq. (3), V, ${C_T}^2$, C_L and C_D are supposed to be constant. Nevertheless, the aircraft changes its attitude during cruise, if speed and height are constant. For this reason, it is important to focus the attention on the differential formulation of the Eq. (3).

$$C_L = \frac{W}{\frac{1}{2}\,\rho\,V^2 S} \quad \Rightarrow \quad \mathrm{d}R = \frac{V}{c_T}\frac{1}{C_D}\frac{W}{\frac{1}{2}\,\rho\,V^2 S}\frac{1}{W}\,\mathrm{d}W = \frac{2}{c_T\,\rho\,V\,S}\frac{1}{C_D}\mathrm{d}W \tag{4}$$

Integrating Eq. (4) between the initial W_{in} and the final aircraft weight W_{fin}, it becomes:

$$R = \frac{2}{C_T\,\rho\,V\,S}\int_{W_{fin}}^{W_{in}}\frac{1}{C_D}\mathrm{d}W \tag{5}$$

To evaluate the integral in Eq. (5), a relation $C_D = C_D\,(W)$ is needed. Nevertheless this is not linear and not known *a priori* and the aim to find an analytical solution is not effective.

[1]We are supposing that all the stringers are identical for each section. The same hypothesis is applied to spar webs and to skin panels.

[2]In this work C_T is always supposed to be constant.

Eq. (3) can be detailed as follows:

$$R = \frac{V}{c_T}\frac{C_L}{C_D}\ln\left(\frac{W_{stru}+W_{const}+W_{fuel}}{W_{stru}+W_{const}}\right) \tag{6}$$

where W_{stru} is the structural weight, W_{const} is the constant weight and includes: engines, avionics, passengers, fuel for climb and descent, etc., and W_{fuel} is the weight of the fuel can be used for the cruise. Terms affected by the optimization process are C_D and W_{stru}.

Instead of considering a fully constant step range that represents a too strong approximation, let us suppose to divide the fuel consumption into several steps.

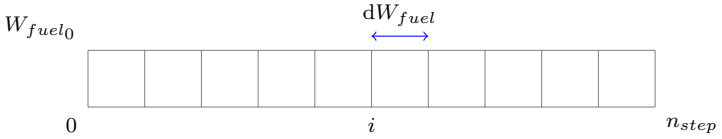

Figure 2: Fuel discretization.

Fig. 2 shows how the fuel for the cruise is divided. Where W_{fuel_0} is the total fuel for the cruise only, n is the step number and $\mathrm{d}W_{fuel} = \frac{W_{fuel_0}}{n}$ is the fuel consumption of each step. Following this approach it is possible to define a *piecewise* constant step range formula, considering a fixed attitude for each single step.

In this case, Eq. (6) can be rearranged in this way:

$$R^{(i+1)} = \frac{V}{c_T}\frac{C_L^{(i)}}{C_D}\ln\left(\frac{W_{stru}+W_{const}+W_{fuel}^{(i)}}{W_{stru}+W_{const}+W_{fuel}^{(i+1)}}\right) \tag{7}$$

with $W_{fuel}^{(i)} = W_{fuel_0} - i\ \mathrm{d}W_{fuel}$ and $i = 0 : n-1$

$$C_L^{(i)} = \frac{W_{stru}+W_{const}+W_{fuel}^{(i)}}{\frac{1}{2}\rho\ V^2 S} \tag{8}$$

Eq. (8) shows that the angle of attack of each step, $\alpha^{(i)}$, is fixed at its beginning. The more the steps are considered, the more accurate the range evaluation is.

3.2 Aerostructural optimization

In general the objective function of a multidisciplinary problem depends not only on the design variables, but also on the physical state variables. So, if the vector of design variables is $\boldsymbol{x}$ and the vector of physical state variables is $\boldsymbol{y}(\boldsymbol{x})$, the objective function $\mathcal{I}$ can be defined as $\mathcal{I} = \mathcal{I}(\boldsymbol{x},\ \boldsymbol{y}(\boldsymbol{x}))$. The objective function, i.e. the range, must be maximized subjected to a set of inequality constraints: $\boldsymbol{g}(\boldsymbol{x},\ \boldsymbol{y}(\boldsymbol{x})) \leq \boldsymbol{0}$. So the optimization problem is summarized as follows:

$$\begin{cases} \min\limits_{\boldsymbol{x}} \mathcal{I}\left(\boldsymbol{x},\ \boldsymbol{y}\left(\boldsymbol{x}\right)\right) \\ \boldsymbol{g}\left(\boldsymbol{x},\ \boldsymbol{y}\left(\boldsymbol{x}\right)\right) \leq \mathbf{0} \end{cases} \tag{9}$$

$$\mathcal{I} = R = R\left(C_D, W\right) = R\left(C_D\left(\boldsymbol{x}, W\left(\boldsymbol{x}\right)\right), W\left(\boldsymbol{x}\right)\right) \tag{10}$$

The derivative of the objective function $\mathcal{I}$ w.r.t the set of design variables $\boldsymbol{x}$ becomes:

$$\frac{\mathrm{d}\mathcal{I}}{\mathrm{d}\boldsymbol{x}} = \frac{\mathrm{d}R}{\mathrm{d}\boldsymbol{x}} = \frac{\partial R}{\partial C_D}\frac{\mathrm{d}C_D}{\mathrm{d}\boldsymbol{x}} + \frac{\partial R}{\partial W}\frac{\mathrm{d}W}{\mathrm{d}\boldsymbol{x}} \tag{11}$$

Since C_D depends on both design variables $\boldsymbol{x}$ and aircraft weight W, while W depends only on design variables, Eq. (11) becomes:

$$\frac{\mathrm{d}R}{\mathrm{d}\boldsymbol{x}} = \underbrace{\frac{\partial R}{\partial C_D}}_{\alpha_{\mathcal{A}}}\frac{\partial C_D}{\partial \boldsymbol{x}} + \underbrace{\left(\frac{\partial R}{\partial C_D}\frac{\partial C_D}{\partial C_L}\frac{\partial C_L}{\partial W} + \frac{\partial R}{\partial W}\right)}_{\alpha_{\mathcal{S}}}\frac{\mathrm{d}W}{\mathrm{d}\boldsymbol{x}}$$

where $\alpha_{\mathcal{A}}$ and $\alpha_{\mathcal{A}}$ can be compiuted analytically.

Applying the penalty method to the problem of Eq. (9) for the constraints, it results: $\mathcal{J}\left(\boldsymbol{x},\ \boldsymbol{y}\left(\boldsymbol{x}\right)\right) = \mathcal{I} + \frac{1}{2}\ \boldsymbol{g}^T\mathbf{P}\boldsymbol{g}$. Splitting the design variables in aerodynamics $\boldsymbol{x}_{\mathcal{A}}$ and structures $\boldsymbol{x}_{\mathcal{S}}$, and considering both aerodynamic $\boldsymbol{g}_{\mathcal{A}}$ and structural $\boldsymbol{g}_{\mathcal{S}}$ constraints, the derivative of $\mathcal{J}$ is:

$$\begin{aligned} \frac{\mathrm{d}\mathcal{J}}{\mathrm{d}\boldsymbol{x}} &= \begin{bmatrix} \frac{\mathrm{d}\mathcal{I}}{\mathrm{d}\boldsymbol{x}_{\mathcal{A}}} & \frac{\mathrm{d}\mathcal{I}}{\mathrm{d}\boldsymbol{x}_{\mathcal{S}}} \end{bmatrix} + \begin{bmatrix} \boldsymbol{g}_{\mathcal{A}}^T & \boldsymbol{g}_{\mathcal{S}}^T \end{bmatrix}\mathbf{P}\begin{bmatrix} \frac{\mathrm{d}\boldsymbol{g}_{\mathcal{A}}}{\mathrm{d}\boldsymbol{x}_{\mathcal{A}}} & \frac{\mathrm{d}\boldsymbol{g}_{\mathcal{A}}}{\mathrm{d}\boldsymbol{x}_{\mathcal{S}}} \\ \frac{\mathrm{d}\boldsymbol{g}_{\mathcal{S}}}{\mathrm{d}\boldsymbol{x}_{\mathcal{A}}} & \frac{\mathrm{d}\boldsymbol{g}_{\mathcal{S}}}{\mathrm{d}\boldsymbol{x}_{\mathcal{S}}} \end{bmatrix} \\ &= \alpha_{\mathcal{A}}\begin{bmatrix} \frac{\mathrm{d}C_D}{\mathrm{d}\boldsymbol{x}_{\mathcal{A}}} & \frac{\mathrm{d}C_D}{\mathrm{d}\boldsymbol{x}_{\mathcal{S}}} \end{bmatrix} + \alpha_{\mathcal{S}}\begin{bmatrix} \frac{\mathrm{d}W}{\mathrm{d}\boldsymbol{x}_{\mathcal{A}}} & \frac{\mathrm{d}W}{\mathrm{d}\boldsymbol{x}_{\mathcal{S}}} \end{bmatrix} + \begin{bmatrix} \boldsymbol{g}_{\mathcal{A}}^T & \boldsymbol{g}_{\mathcal{S}}^T \end{bmatrix}\mathbf{P}\begin{bmatrix} \frac{\mathrm{d}\boldsymbol{g}_{\mathcal{A}}}{\mathrm{d}\boldsymbol{x}_{\mathcal{A}}} & \frac{\mathrm{d}\boldsymbol{g}_{\mathcal{A}}}{\mathrm{d}\boldsymbol{x}_{\mathcal{S}}} \\ \frac{\mathrm{d}\boldsymbol{g}_{\mathcal{S}}}{\mathrm{d}\boldsymbol{x}_{\mathcal{A}}} & \frac{\mathrm{d}\boldsymbol{g}_{\mathcal{S}}}{\mathrm{d}\boldsymbol{x}_{\mathcal{S}}} \end{bmatrix} \end{aligned} \tag{12}$$

The gradient based optimization algorithm starting from an initial guess, looks for a better solution in the design space moving in the opposite direction of the gradient of the function which has to be minimized, i.e.

$$\boldsymbol{x}^{(n+1)} = \boldsymbol{x}^{(n)} - \Gamma\left.\frac{\mathrm{d}\mathcal{J}}{\mathrm{d}\boldsymbol{x}}\right|_n \tag{13}$$

3.3 Problem set up

The first iteration of the optimization process is shown in Fig. 3 and it is performed out of the optimization loop. It consists of three blocks, whose objective is to evaluate the static aeroelastic shape of the wing.

Figure 3: First iteration.

The procedure is a static aeroelastic calculation and can be summarized in the following steps: first, a direct aerodynamics analysis is performed. The aerodynamic loads are then transfered to the structural solver. Once the deformed geometry is known, a new mesh for the aerodynamic computation is produced by the mesh generator. Hence, the static aeroelastic shape of the wing is used as baseline geometry for the optimization problem.

Fig. 4 shows the block diagram that represents the single objective optimization process. It is possible to distinguish four main parts that constitute it: an initial structural analysis, the aerodynamic calculations, the geometric evaluation and a final structural analysis.

The initial structural analysis is performed to obtain the current structural weight of the wing. Thanks to this information, the total lift coefficient is calculated and is then used in the CFD analysis in order to trim the aircraft. The aerodynamic part is composed by several calculations. A direct CFD calculation to have the complete aerodynamic solution is used to perform the adjoint analysis. Other two direct calculations are performed at different lift coefficients to evaluate the aerodynamic performance about of the trim point. Then, a geometric evaluation is executed in order to check if the thickness constraints are satisfied and to provide their sensitivities with respect to the aerodynamic design variables. A second structural analysis evaluates the structural sensitivities. All the sensitivities are collected inside the derivative map, where they are manipulated to obtain the cross derivatives.

The derivative map is used by the optimizer to perform the gradient-driven optimization. A new set of design variables is produced and the optimization loop is repeated until one of the convergence criteria is satisfied.

The extension to multiple objective optimization is straightforward. The multi-objective function is a blend of several single-objective functions. As already discussed, the idea is to divide the entire cruise into a certain number of steps and to maximize the feasible range for each step simultaneously. Hence, the multi-objective function is defined as:

$$R = R_1 + \cdots + R_{n_{step}} = \sum_{i}^{n_{step}} R_i \tag{14}$$

where R_i, with $i = 1 : n_{step}$, represents a portion of the entire cruise range and n_{step} is the number of steps. Consequently, it is necessary to calculate all the parameters for each configuration. A preliminary iteration is needed to evaluate the static aeroelastic shape of the wing for each configuration (Fig. 3).

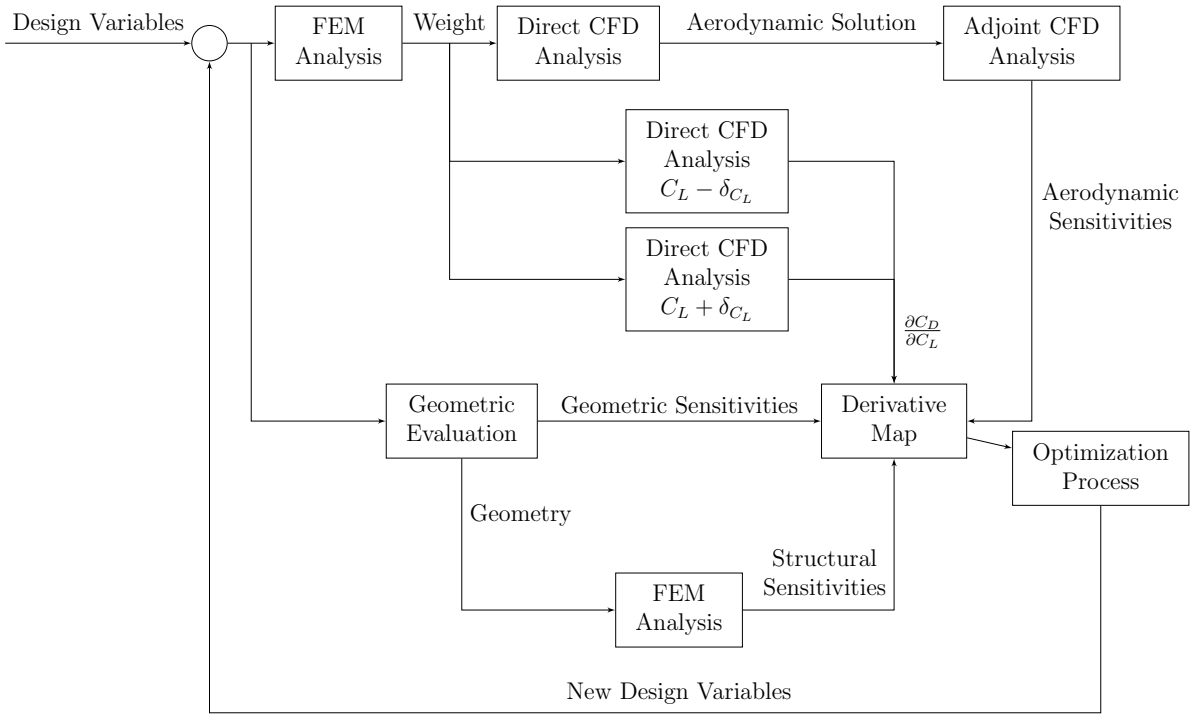

Figure 4: Block diagram for single objective optimization process.

Once all the configurations are evaluated (basically repeating the process resumed in Fig. 4), data are collected and recombined in order to obtain the objective function and the derivative map, which are then sent to the optimization software (Fig. 5). In order to limit the computational cost, if more than three configurations are considered, the recombine block is used to interpolates with respect to all parameters.

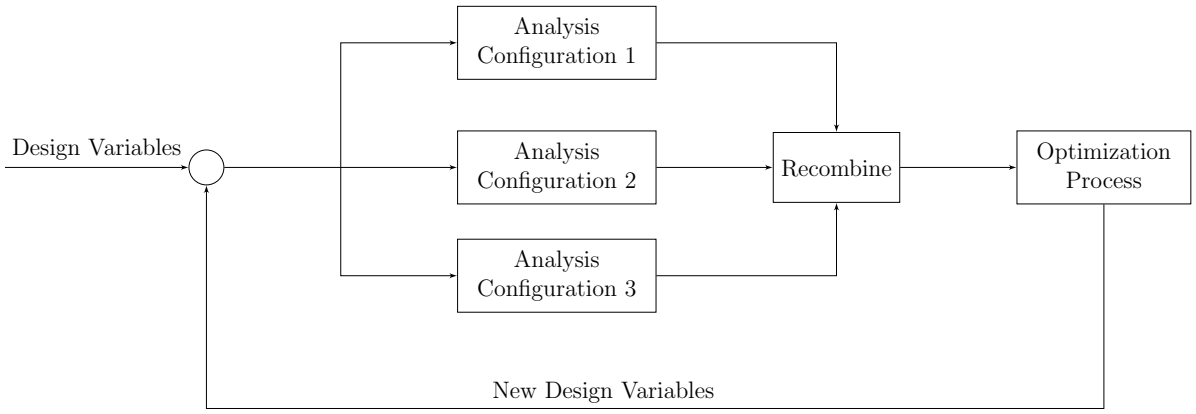

Figure 5: Block diagram for multiple objective optimization process.

4 Management of constraints

Several techniques are available in literature to handle inequality constraints for an optimization problem. In the following we briefly describe the methods that are currently used.

The method used in this optimization process is the penalty method. It consists in adding a penalty term to the objective function, composed by the constraint parameter and a weight term. This indicates how much the constraint can be violated. The aerostructural optimization has been performed imposing the lift coefficient with an equality constraint, while the moment coefficient with an inequality constraint. The thickness has been evaluated at some points along the wing span and chord-wise and controlled with inequality constraints. A

For the structural constraints to limit the computational cost and simplify the management of the problem, it has been decided to adopt the Kreisselmeier-Steinhauser (KS) Method [3]. The KS function uses a "draw-down" factor or aggregation parameter, ρ, which is analogous to the penalty factor in the penalty methods.

The KS function can be used to aggregate the constraints into a single composite function. Suppose that we have the following constraint for each structural finite element:

$$g_m(\boldsymbol{x}) = 1 - \frac{\sigma_m(\boldsymbol{x})}{\sigma_y} \geq 0 \tag{15}$$

where σ_m is the von Mises stress in element m and σ_y is the yield stress of the material. The corresponding KS function is defined as:

$$KS(\mathbf{g}(\boldsymbol{x})) = -\frac{1}{\rho}\ln\left(\sum_m e^{-\rho g_m(\boldsymbol{x})}\right) \geq 0 \tag{16}$$

This function represents a lower bound envelope of all of the constraint inequalities, where ρ is a positive parameter that express how close this bound is to the actual minimum of the constraints. This constraint lumping method is conservative and might not achieve the same results as managing each stress constraints separately. However, the use of KS functions is a viable alternative, being effective in optimization problems with thousands of constraints.

In the problem considered it is necessary to handle a large number of structural constraints so Kreisselmeier-Steinhauser approach with a value of the aggregation parameter equal to $\rho = 200$ has been adopter.

5 RESULTS

5.1 Single-objective optimizations

Fig. 6 compares the contour of the Mach number on the initial and on the optimized wing obtained with the coupled and the uncoupled optimization processes.

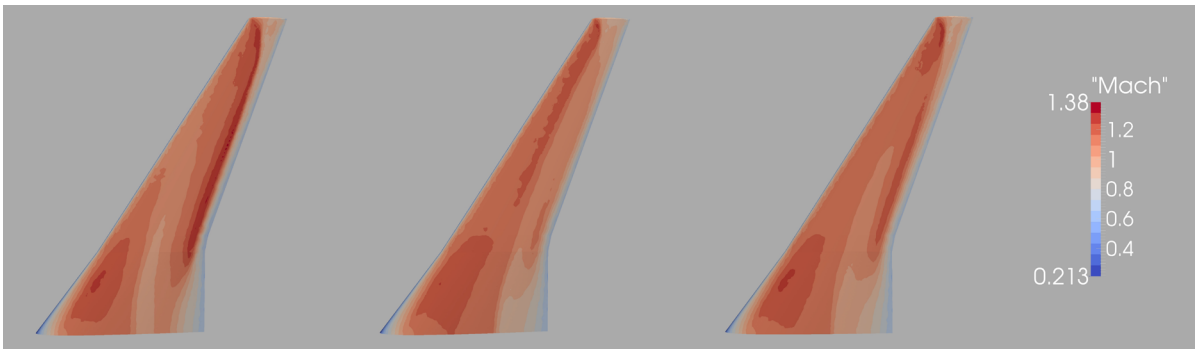

Initial Coupled Uncoupled

Figure 6: Contour of the Mach number on the initial (left) and optimized coupled (center) and uncoupled (right) wing.

The initial wing is characterized by a strong shock located in the aft part of the wing that runs along the 80% of the wing span and a supersonic bubble located in the front part of the wing. The optimized wing obtained from coupled optimization (Fig. 6) shows a weaker shock that moves forward, toward the leading edge. The flow never exceeds Mach 1.2, preventing the buffet onset. There is a small speed up area beyond the shock that affects the aerodynamic performance in a negative way while, the supersonic bubble is flattened down.

The optimized wing obtained from the uncoupled optimization is characterized by a weaker shock than the original wing but it does not move forward, causing a rapid re-compression of the flow near the trailing edge. The flow remains essentially unvaried near the wing tip, possibly causing buffet onset. The supersonic bubble does not change position or intensity.

From the structural point of view, the resistance section of the different structural components has been reduced in order to exploit completely the mechanical properties of the material, leading to an important reduction in the mass of the aircraft (Tab. 3).

Optimization	**Mass (kg)**	**Variation (%)**
Coupled	-187	-16.97
Uncoupled	-183	-16.60

Table 3: Mass variation with respect to the initial wing.

5.2 Multi-objectives optimizations

Two different multi-objective optimizations have been performed. The first one considers three steps in the cruise range, while the second one considers nine steps. In the

second case, to reduce the computational cost only three CFD calculations were performed, interpolating the results for the other steps. The aerodynamic results show an improvement of the performance in both cases. They are summarized in the polar curves (Fig. 7) in the comparison paragraph.

5.3 Comparison

In this section a comparison among all the optimized wings and the initial one is presented.

The comparison of the polar curves is shown in Fig. 7. Both the coupled and the uncoupled wings show a regular and smooth polar curve. The multi-point wings have a particular trend. Starting from the beginning of the cruise, the two curves run in parallel. When they reach $C_L = 0.3$ they distance themselves. Actually, the three-point wing drops at a lower C_D than the nine-point one. After this jump, they almost touch and proceed together. We have to point out that the three-point wing has a better behavior outside the cruise range of points.

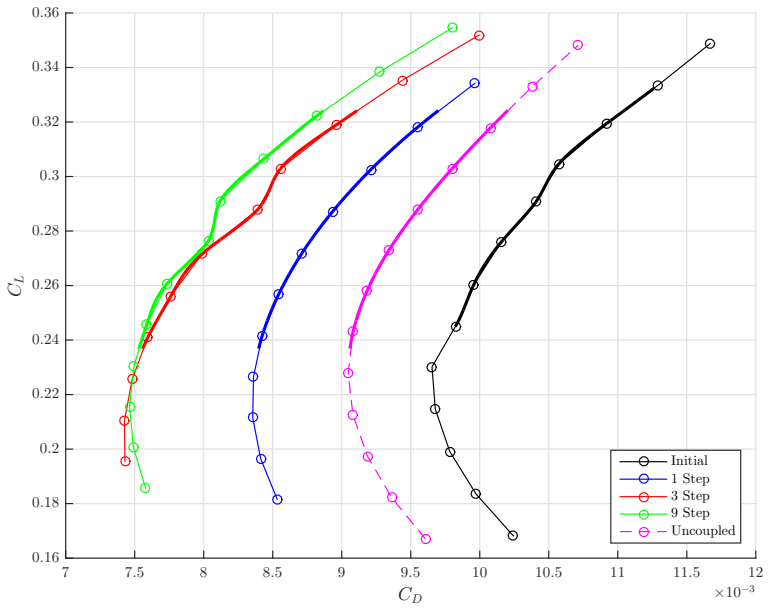

Figure 7: Comparison of the polar curves.

Tab. 4 lists the total range values and the increment with respect to the initial wing.

Wing Geometry	**Total Range** (km)	**Increment** (%)
Initial	5926	
Uncoupled	6482	9.38
Coupled	6924	16.84
Three-Point	7513	26.78
Nine-Point	7647	29.04

Table 4: Total range and percent increment.

6 CONCLUSIONS

The available literature about MDO applied to aircraft design uses the Breguet range equation as objective function. This means that the variation of attitude during cruise, which is related to the loss of weight caused by fuel consumption, is not taken into account. The innovative approach presented in this thesis is to divide the cruise into a certain number of steps; over each step the attitude is considered to be constant, so that the Breguet range formula can be applied. The total range is then evaluated as the sum of the ranges of each step, leading to a sort of multi-objective optimization. The bigger is the number of step considered, the more accurate is the solution obtained. This new approach is called "step-range" and its results are compared with those obtained through sequential discipline optimization and single objective optimization.

Therefore, four different optimization tasks have been performed and the results demonstrate that the method we developed is successful when applied to our specific case. In particular, comparing the results obtained from the single-objective optimizations, we can notice that the coupled technique leads to a larger improvement than the uncoupled one.

Both the three and the nine-point optimizations lead to better results than the single-objective one. As expected, enlarging the number of evaluation along the cruise, the objective function, seen as the sum of sub-functions, increases its value.

The nine-point optimization turns out to be the best procedure in absolute terms, highlighting the effectiveness of the subdivision in different steps of the cruise. Actually, this allows to consider the variation of the aircraft attitude during the cruise. Moreover, we are able to demonstrate that the spline interpolation of the optimization parameters (i.e. objective function, constraints and gradients) leads to a reduction of the computational cost, ensuring, at the same time, accurate results.

The growth of the number of evaluations over the cruise also causes the increase of the number of iterations needed for the optimization process to converge. This could represent a limitation of the number of evaluation points that can be used. Heuristically speaking, the undefined increase of evaluation points would lead to a robust optimization, whose intent is the maximization of the mean value of the objective function, minimizing its standard deviation.

REFERENCES

[1] J. Sobieszczanski-Sobieski and R. T. Haftka. Multidisciplinary aerospace design optimization: survey of recent developments. *Structural optimization*, 14(1):1–23, 1997.

[2] Joaquim RRA Martins and Andrew B Lambe. Multidisciplinary design optimization: a survey of architectures. *AIAA journal*, 51(9):2049–2075, 2013.

[3] G. Kreisselmeier and R. Steinhauser. Systematic control design by optimizing a vector performance index. *International Federation of Active Controls Syposium on Computer-Aided Design of Control Systems, Zurich, Switzerland*, 1979.

[4] Gaetan KW Kenway and Joaquim RRA Martins. Multipoint high-fidelity aerostructural optimization of a transport aircraft configuration. *Journal of Aircraft*, 51(1):144–160, 2014.

[5] Olivier Pironneau. On optimum design in fluid mechanics. *Journal of Fluid Mechanics*, 64(1):97–110, 1974.

[6] Antony Jameson. Aerodynamic design via control theory. *Journal of Scientific Computing*, 3(3):233–260, 1988.

[7] Jamshid Samareh. Aerodynamic shape optimization based on free-form deformation. In *10th AIAA/ISSMO Multidisciplinary Analysis and Optimization Conference*, page 4630, 2004.

[8] Toni Lassila and Gianluigi Rozza. Parametric free-form shape design with pde models and reduced basis method. *Computer Methods in Applied Mechanics and Engineering*, 199(23):1583–1592, 2010.

[9] Jamshid A Samareh. Survey of shape parameterization techniques for high-fidelity multidisciplinary shape optimization. *AIAA journal*, 39(5):877–884, 2001.

[10] John D Anderson. *Introduction to Flight*. Mc Graw-Hill International Editions, Aerospace Science Series, 1989.